PCCP

Accepted Manuscript

ROYAL SOCIETY OF CHEMISTRY

www.rsc.org/pccp

Effect of molecular level dispersion of Graphene Oxide on free volume characteristics of Poly(vinyl alcohol) and its impact on thermal and mechanical properties of their nanocomposites

S. K. Sharma[†], J. Prakash[‡], P. K. Pujari[*†]

[†]Radiochemistry Division, [‡]Powder Metallurgy Division, Bhabha Atomic Research Centre, Trombay, Mumbai 400085, India

Corresponding Author
Email: pujari@barc.gov.in
Phone: 91-22-25595326
Fax: 91-22-25505151

Abstract

Poly(vinyl Alcohol), PVA, reinforced with carbon nanofillers has shown drastic variations in thermal as well as mechanical properties. In order to establish structure-property correlations, these variations have been correlated to the modifications in hydrogen bonding structure as well as crystallinity of PVA matrix without paying much attention to molecular packing in the amorphous region of this semicrystalline polymer. In order to investigate the molecular packing in PVA-graphene oxide (GO) nanocomposites, free volume characterization of PVA-GO nanocomposites has been carried out using *ortho*-positronium (*o*-Ps) probe. The variations in free volume size, density and size distribution have been determined through *o*-Ps lifetime and corresponding intensity as well as its lifetime distribution. The variation in hydrogen bonding and its effect on crystallinity has been determined by Fourier Transformed Infra Red (FT*IR*) and X-ray diffraction (XRD) measurements. The variation in thermal (glass transition temperature) and mechanical (Young's Modulus, tensile strength and percentage strain at break) properties of the nanocomposites are explained in view of free volume structure and crystallinity of PVA matrix which are severely modified due to molecular-level dispersion of GO sheets in PVA matrix.

1. Introduction

In order to make polymer nanocomposites with hydrophilic nanofillers, Poly (vinyl alcohol), PVA, has remained a promising choice. This is primarily due to the hydroxyl groups present in PVA backbone which facilitates the molecular level dispersion of nanofillers by interacting with them through hydrogen bonding. PVA has wide range applications in textile and adhesives, coating materials, functional membranes, drug delivery and fuel cells mainly due to its biocompatibility, water solubility and hydroxyl fill nature. In literature, PVA based polymer nanocomposites have shown a drastic variation in its thermal and mechanical properties depending on the type of nanofillers and the preparation method of the nanocomposites.[1-16] For example, Zhang et al.[1] have reported 64.9 and 77.4% increase in tensile modulus and tensile strength, respectively using water dispersible graphene sheets stabilized by multiwall carbon nanotubes (MWCNTs) as filler. Similarly Xu et al.[4] have reported an increase of 190 % in tensile modulus by incorporating 5wt.% of layered graphene oxide (GO) in PVA matrix. Bao et al.[6] has also shown an increase in tensile modulus and tensile strength by incorporating GO and graphene in PVA matrix. They have also shown that along with mechanical properties, the glass transition temperature (T_g) is also changed due to incorporation of these fillers in PVA matrix. The T_g was shown to increase with GO loading while a decrease in T_g is observed on incorporation of graphene in PVA matrix.

Various types of nanofillers such as metal and metal oxide nanoparticles, clays, silica, layered double hydroxide and carbon based nanofillers have been used to reinforce the PVA matrix. Carbon based nanofillers such as multiwall and single wall carbon nanotubes (CNTs), GO and reduced GO (r-GO) etc. have received enormous attention mainly due to their great mechanical, thermal and electrical properties. For example, the Young's modulus and tensile stress of single wall carbon nanotubes and GO can attain (1 TPa, 180 GPa) and (250GPa, 60GPa) values, respectively.[17-19] Among carbon based nanofillers, carbon nanotubes (CNTs) have attained intense attention for the reinforcement of polymer matrices but limited enhancement have been achieved in the bulk physical properties. This is mainly due to the aggregation of CNTs in polymer matrix. The aggregation of CNTs occurs due to non availability of functional groups at its surface which prevents any chemical interaction of CNTs with polymer molecules. In order to prevent the aggregation, surface modifications of CNTs with polymer compatible functional groups was shown to be a promising method. Using this approach, CNTs can

be well dispersed in polymer matrices at higher concentration but again limited enhancement was achieved in bulk physical properties. This is primarily because the structure of CNTs is impaired due to functionalization process and as a result physical properties of the formed composite suffer.[7,12] Same phenomenon is true for graphene which is sp^2 bonded single atom layer thick two dimensional carbon sheet. The main challenge remains exactly the same i.e. exfoliation and dispersion of the nanofillers as graphene undergoes stacking due to strong intrinsic van der Waal interactions. Among all these carbon based nanofillers, recently GO has received enormous attention primarily due to its easy production at large scale, availability of functional groups and its comparable intrinsic properties. Enormous variation in thermal and mechanical properties of PVA-GO nanocomposites have been reported.[3-6,13-16,20] These variations in physical properties are the result of enhanced interaction between GO and PVA molecules through hydrogen bonding. The hydrogen bonding facilitates the GO dispersion in PVA matrix which consequently improves the load transfer from PVA molecules to GO. In literature, main focus has remained on PVA-GO interaction and dispersion of GO while not much attention has been paid to the changes in structure of PVA matrix as a result of GO loading. The PVA matrix in these nanocomposite occupy large volume fraction (~ 100% at very low loading) and any modification in PVA matrix is expected to play a deterministic role in the evolved properties. In literature, only crystallinity measurements have been used as an index to verify the intrinsic properties of PVA matrix. The newly formed hydrogen bonds between PVA and GO might alter the original hydrogen bonded structure within amorphous region of PVA matrix leading to changes in molecular packing of PVA. PVA is a semicrystalline polymer and its properties, in addition to crystallinity, are heavily dependent on its molecular packing in amorphous region but it has been underplayed in most of the studies. Free volume holes in amorphous region can be indexed to measure the changes in molecular packing at sub nanolevel.

Positron annihilation lifetime spectroscopy (PALS) is a well established technique for measuring the free volume size, density and its size distribution in the polymer nanocomposites.[21-28] Followed by implantation of positrons from a radioactive source (^{22}Na) in polymer nanocomposites, a fraction of thermalized positrons forms a quasi bound state, positronium (Ps), with an electron. The positronium can occur in two different states depending on the spin orientation of electron and positron. The singlet spin state (anti-parallel spin), *para*-positronium, (*p*-Ps) and triplet spin state (parallel spin), *ortho*-positronium, (*o*-Ps) are produced with relative abundance of 1:3 and their

intrinsic lifetimes are 125 ps and 142 ns, respectively. In polymer nanocomposites, the trapped Ps from free volume holes may annihilate via an additional mode wherein it annihilates with an opposite spin electron from the surrounding atoms. The process is called *pick-off* annihilation and as a result, the *o*-Ps lifetime reduces from 142 ns to 1-10 ns. The extent of reduction depends on the size of free volume holes. Under the assumption of spherical free volume holes to be a finite potential well wherein *o*-Ps atoms is trapped, the *o*-Ps *pick-off* lifetime, τ_3 (ns), in a polymer is correlated with the radius (R, nm) of free volume holes using the Tao-Eldrup equation[29,30]

$$\tau_3 = \frac{1}{2}\left[1 - \frac{R}{R+\Delta R} + \frac{1}{2\pi}\sin\left(\frac{2\pi R}{R+\Delta R}\right)\right]^{-1} \quad (1)$$

where ΔR = 0.166 nm is an empirical parameter determined using materials with well known size of free volume holes. The corresponding intensity, I_3, is related to the fractional free volume assuming that no other chemical species is present in the matrix which can inhibit/quench the positronium formation. A distribution over *o*-Ps lifetime is measured to determine the free volume hole size distribution in the polymer nanocomposites. Recently, we have shown that positron and positronium are also efficiently trapped at the free volume nanoholes available at the polymer-nanofillers interface which enables the characterization of evolved nanostructure of the polymer composites.[21-25] The conventional techniques like X-ray diffraction (XRD), Fourier transform infra-red (*FT*IR), Thermal gravimetric analysis (TGA), Differential scanning calorimetery (DSC) and Dynamical mechanical analysis (DMA) are used to infer the changes in polymer structure. The electron microscopy techniques can provide direct information about the structure of polymer nanocomposite but these require special methods for sample preparations. PALS measurements do not require any special methods for sample preparation and can provide direct information about the changes in the free volume structure (sub nanolevel) which is not possible by other techniques. Hence, PALS can provide unique information about the free volume structure of polymer nanocomposites which is expected to have significant role in governing their bulk physical properties.

In the present study, we have investigated the free volume characteristics (free volume size, density and size distribution) of PVA-GO (0.25, 0.50, 1.0 and 2.0 GO *wt.*% GO) at room temperature using PALS. The hydrogen bonding between PVA molecules and GO has been indexed using *FT*IR measurements. The changes in crystallinity as a result of the nanocomposite formation have been determined using XRD. Scanning electron

microscopy (SEM) has been used to capture the fractured surface morphology of the composite films which provides supplementary information on mechanical properties through fracture mechanism. The modifications in thermal properties (T_g) and mechanical properties (Young's modulus, tensile strength and percentage strain at failure) have been explained in view of the changes in free volume characteristics, crystallinity and hydrogen bonded structure of PVA.

2. Experimental

2.1. Preparation of PVA-GO Nanocomposites

GO powder was synthesized by electrochemical exfoliation of commercial graphite. Graphite rods (length: 150 mm, diameter: 6 mm, 99.995% trace metals basis) were used as the starting material. Activation of graphite rod was carried out by immersing it in a bath of 98% concentrated sulfuric acid for 2 hours prior to electrochemical exfoliation process. The activation process forces the crystal lattice planes apart leading to an increased interlayer spacing as a result of reduction in the van der Waals forces between the adjacent carbon sheets. In a typical electrochemical exfoliation process, the activated graphite rod was used as anode in an electrolysis cell filled with 0.5 M Sulfuric acid aqueous solution. A constant potential of 7 V was applied to the anode with respect to the cathode. GO layers were gradually exfoliated from the activated graphite anode rod and dispersed in the aqueous solution. The solution with dispersed GO layers was subsequently taken from the electrolysis cell. This solution was centrifuged at 6000 rpm for 10 min (5 cycles) to remove large aggregates. The supernatant was decanted and the GO powder was obtained by filtering the solution using PVDF membrane. The GO powder was again transferred to water and thus obtained brown colour aqueous solution was used for the preparation of PVA nanocomposites. The GO aqueous solution shows long durability as no aggregation is observed even after 2-3 weeks.

PVA-GO nanocomposite films were prepared using simple solution mixing method. For the preparation, 5g of PVA (average M.W. 89000-98000, more than 99% hydrolyzed) was dissolved in 20 ml of deionized water to form polymer solution. Appropriate amount of GO solution was added to the aqueous PVA solution maintained at 90^{o}C under ultrasonication. After few hours of ultrasonication, the mixture was stirred for 6 hours at 90^{o}C. The solution was cast on extremely clean aluminium mould kept at

room temperature. The nanocomposite films were dried in vacuum oven at 60°C for 4-5 hours and stored in a vacuum desiccator. The nanocomposite films with (0.25, 0.50, 1.0 and 2.0 *wt.*% GO) were prepared using the described method. These samples are further noted as PVA*x*GO where value of *x* is the weight percent of GO. The thickness of the films was ~ 100 μm measured using digital micrometer. Thus produced films were free from air bubbles and could be taken off from aluminium mould easily. In order to remove any adsorbed water from the films before carrying out any measurements, the films were annealed further at 60°C under vacuum for 4-5 hours.

2.2 Characterization of GO and polymer nanocomposites

The GO has been characterized using 2000FX JEOL transmission electron microscope (TEM). The morphology of fractured surface of the nanocomposite films and SEM-energy dispersive X-ray (EDX) spectrum of GO powder have been captured using SEM-Camscan MV2300CT/100, UK. In order to monitor the change in crystallinity, XRD measurements (Philips X pert pro XRD unit) using Cu K_α radiation were carried out. FT*IR* spectra of pure PVA, and nanocomposite films in diffuse reflection mode under vacuum were obtained using Vertex 80v (Bruker) and liquid nitrogen cooled MCT detector from 4000 to 400 cm^{-1} at a resolution of 2 cm^{-1}. The FT*IR* spectrum of GO powder was recorded by making its pellet in dried KBr. The micro laser Raman instrument employed for the present study is Lab Ram HR 800 with a focal length of 800 mm. The laser wavelength used was 514 nm, from an air cooled Argon ion laser of power 30 mW. The GO powder sample was analyzed by Micro-Raman spectroscopic technique. The spectra were recorded in the spectral range of 200–4000 cm^{-1} using a Peltier cooled charge coupled device (CCD) and 1800 line/mm grating. The spectral resolution of the instrument was 1 cm^{-1}.

2.3 Positron annihilation lifetime spectroscopy (PALS)

PALS spectrometer used for the present measurements is a fast-fast coincidence set up coupled to plastic scintillation detectors placed at 180 degree to each other. The time resolution (254 ps) of the spectrometer was measured using ^{60}Co while maintaining the energy windows of discriminators according to prompt gamma (~1274 keV) and annihilation gamma (511 keV) photons from a ^{22}Na positron source. The time calibration of multi channel analyzer (MCA) was 0.0244 ns/channel. The PALS measurements for the nanocomposite samples were carried out under laboratory atmosphere using a

radioactive positron source (^{22}Na, 0.37 MBq) deposited between two kapton films (~7μm thick). In order to ensure the complete positron annihilation within the samples, the source was sandwiched between two stacks (~1.5 mm thick each) of nanocomposite films. The fraction of positrons annihilated within the source and kapton films was evaluated using Si single crystal reference and used as source correction components for analysis of the spectra.

2.4 Thermal properties and Mechanical properties

Thermal gravimetric analysis (TGA) of the nanocomposite films has been carried out using a Netzsch thermobalance under inert atmosphere. The heating rate used for TGA measurement was 10.0 Cmin^{-1}. DSC measurements were carried out in temperature range 28-230^{o}C. The scanning was performed by a METTLER TOLEDO thermal analysis system using argon gas (flow rate 60 mL min^{-1}) in the DSC cell purge. The scanning speed was fixed at 10.0 Cmin^{-1}. The scanning was performed by first heating the sample from 28 to 230 ^{o}C followed by a cooling cycle. Tensile properties of the samples determined using a tensile tester, Autograph AGS-1kND (Shimadzu Co.); the initial length of the specimen was 20 mm, and the extension rate was 2 mm/min.

3. Results

3.1 Characterization of GO

Raman spectra (Figure 1) of GO powder exhibit a strong D-band (~1360 cm^{-1}) and G-band (~1590 cm^{-1}) usually assigned to structural disorder and the graphitized structure respectively. GO presents a dominant D peak arising from the attachment of functional groups such as hydroxyl and epoxy etc. on the carbon skeleton. The D+D' peak (~2950 cm $^{-1}$) represents a defect activated combination of phonons with different moment. The large D–band and the attenuated 2D-band may be attributed to the small sp² domains subsequent to the oxidation process and ultra-sonication during synthesis.

In order to check the exfoliation, TEM images of aqueous GO solution has been taken and shown in figure 2. These images clearly show that GO sheets are well exfoliated in polar solvent. To confirm the presence of functionalities on GO surface, FT*IR* measurements of GO were carried out and the spectrum is shown in figure 3. The characteristic peaks at 3430 cm^{-1}, 1725 cm^{-1} and 1252 cm^{-1} corresponding to –OH and –C=O and –C-O indicates the presence of hydroxyl groups, carbonyl groups and epoxy groups, respectively present at the surface. The SEM-EDX has also been carried out on GO dispersed on a Ta sheet. The SEM micrograph and the EDX spectrum are shown in Figure S1-S2 (*Electronic Supplementary Information, ESI*). The EDX shows the presence

of oxygen with carbon indicating the presence of hydroxyl, epoxy and carbonyl functionalities on carbon surface. In order to prepare the PVA-GO nanocomposite films, thus prepared GO was incorporated in the PVA matrix.

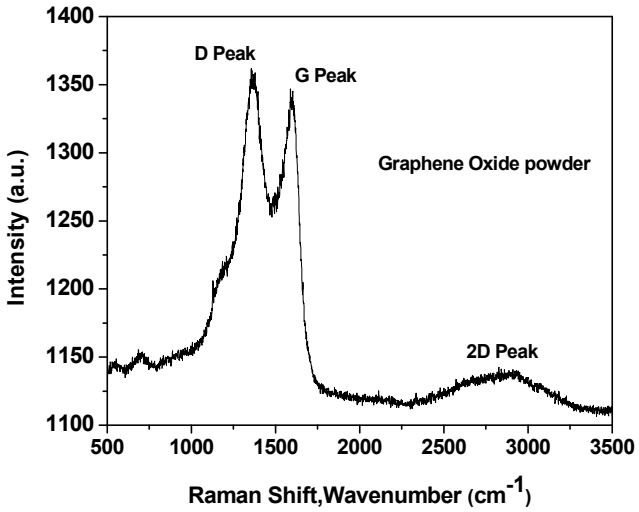

Figure 1. *Raman spectra of Graphene Oxide powder*

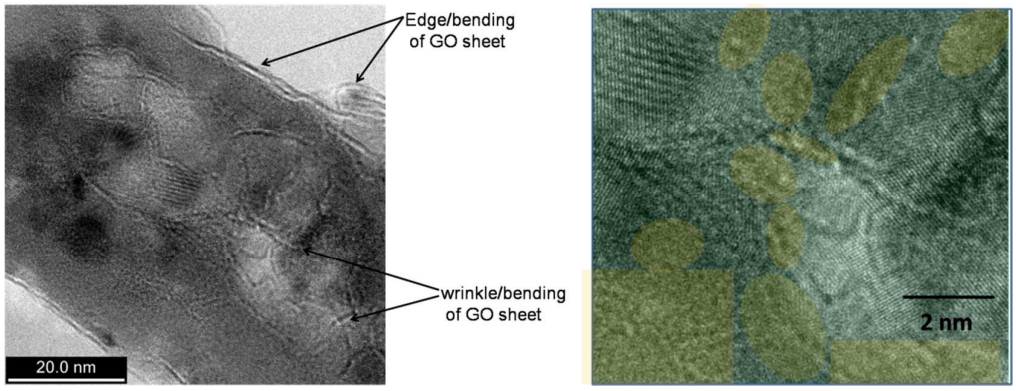

Figure 2. (a) *HRTEM of aqueous suspension of GO showing the edge bending and wrinkle bending of GO* (b) *HRTEM micrograph of GO suspension in ethyl alcohol; greenish region shows the ordered crystalline GO while the yellowish region indicate the presence of amorphous carbon*

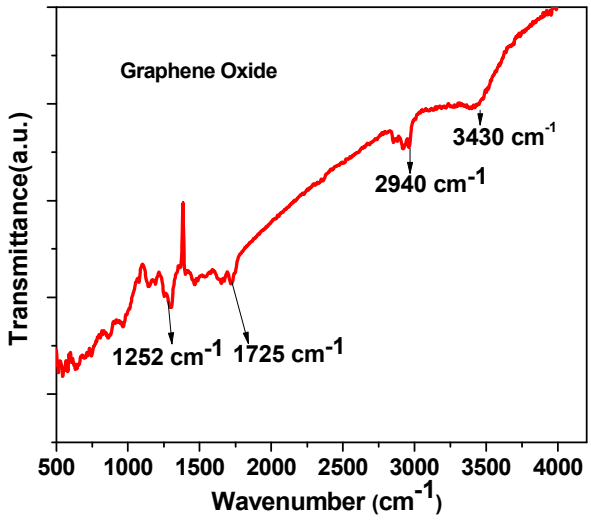

Figure 3. *FTIR of Graphene Oxide powder*

3.2 Mechanical and Thermal properties of PVA-GO Nanocomposites

In order to study the effect of GO incorporation on mechanical and thermal properties of the nanocomposites, mechanical testing, TGA and DSC measurements were carried out. Figure 4 shows the stress vs. strain curves for pure PVA and the nanocomposite films. The figure shows that on incorporation of GO, the nanocomposite films become brittle and undergoes breakdown at lower strain. The mechanical properties such as Young's modulus, Tensile strength and percentage strain at break evaluated from the figure are presented in Table 1. It is observed from the data that all the mechanical properties are hampered due to incorporation of GO in PVA. In literature, various reports are available on PVA-GO nanocomposites where mechanical properties are shown to be enhanced on GO incorporation[1,4,6-8,13-17,20]. The reason behind the deterioration of these properties is discussed in latter section (Discussion). Figure 5 shows the derivative of TGA curves for pure PVA and PVA2.0GO samples, and the inset in the figure shows the mass loss as a function of temperature for the same samples. The derivative curves show three peaks corresponding to mass loss associated with three different processes. The first peak (~ 80^{o}C) is ascribed to absorbed water loss, the second (most prominent ~310^{o}C) peak is ascribed to the loss of –OH functionalities in form of water and the third peak (~430^{o}C) is ascribed to the pyrolisation resulting in production of organic volatiles.[31] The peak position corresponding to a mass loss step provides information about the rate of mass loss for the corresponding process. The peak position temperature values

corresponding to second and third mass loss step (figure 5) for all the samples are reported in Table 1. It is observed from the values that the elimination of water (second step) due to loss of functionalities (-OH) becomes slower on nanocomposite preparation while the loss of organic volatiles (third step) become faster compared to pure PVA. The glass transition temperature (T_g) values determined from the DSC thermogram (Figure 6) is also given in Table 1. The T_g of the nanocomposites are observed to decrease with GO loading in the PVA matrix. As mentioned before, the variation in mechanical and thermal properties are mainly due to the changes in polymer interaction (hydrogen bonding, covalent bonding) with filler, filler dispersion, load transfer from polymer molecules to filler, crystallinity of polymer matrix as well as the molecular packing of the polymer matrix. Among all these, polymer interaction between polymer molecule and filler is most important because many other parameters such as crystallinity, molecular packing and degree of dispersion of fillers also depend on this interaction. In order to elucidate the role of these parameters on the mechanical and thermal properties, PVA nanocomposite films have been characterized for PVA-GO interaction, crystallinity, molecular packing and filler dispersion.

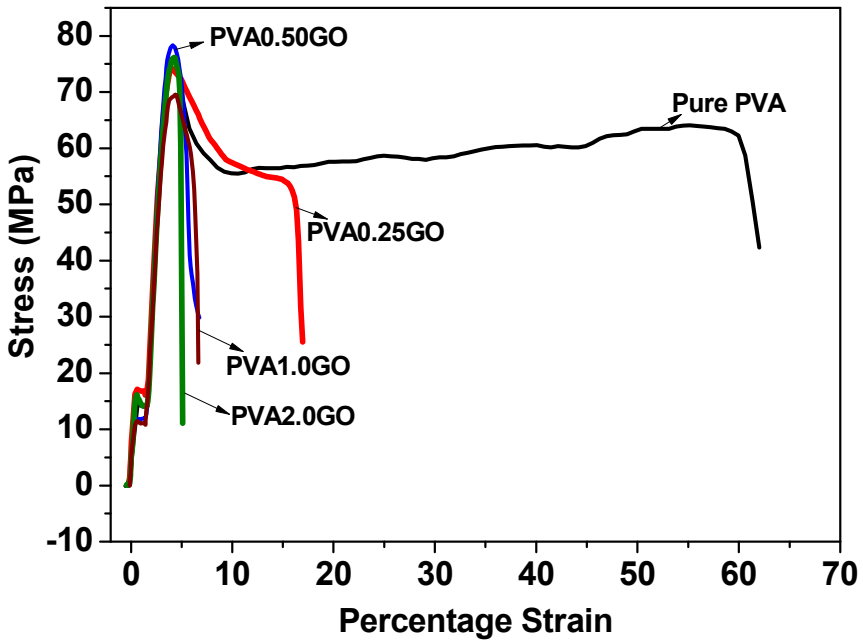

Figure 4. *Stress-Strain curve for pure PVA and PVA nanocomposites*

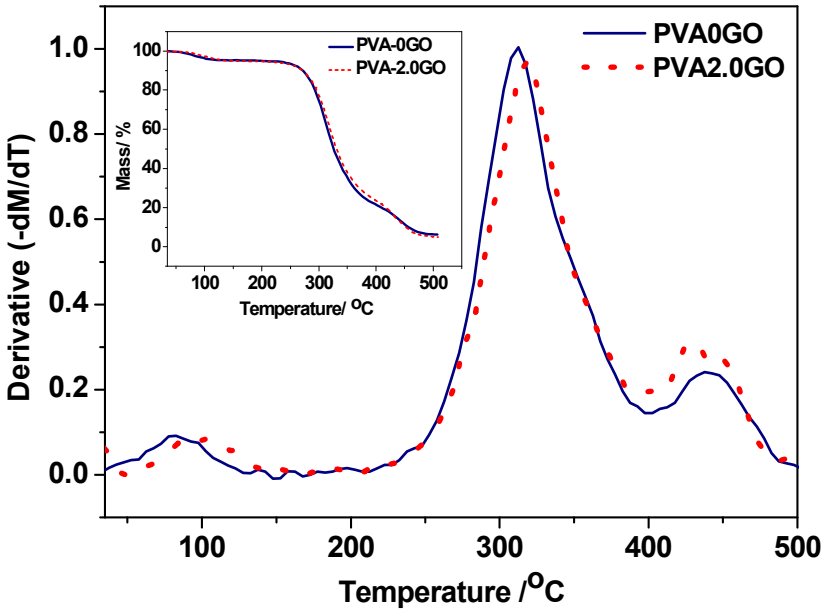

Figure 5. *Derivative of TGA curves for pure PVA and PVA2.0GO; the inset shows the TGA curves for the same samples. For sake of clarity data for only two samples are plotted.*

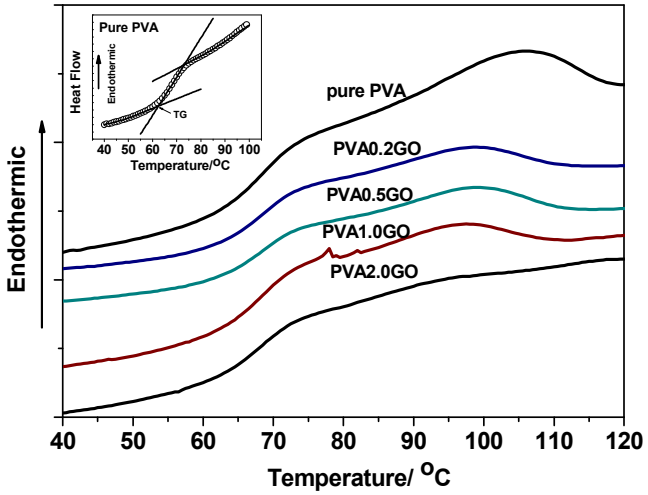

Figure 6. *DSC thermogram showing the glass transition for pure PVA and the nanocomposite films during cooling cycle*

Table 1. *Mechanical and Thermal properties of pure PVA and PVA-GO nanocomposites.*

	Mechanical Testing			TGA		DSC
Sample	**Young's Modulus (GPa)**	**Tensile Strength (MPa)**	**Percentage strain at break**	T_{second} (°C)	T_{Third} (°C)	T_g(°C)
Pure PVA	4.4	77.4	62.4	312.6	437.6	62.4
PVA 0.25	3.8	74.4	17.0	318.0	433.0	61.5
PVA 0.50	4.3	78.3	6.7	319.3	434.3	61.4
PVA 1.0	3.5	69.6	6.7	319.1	430.0	61.2
PVA 2.0	4.0	76.2	5.1	318.9	428.9	60.9

3.3 Characterization of PVA-GO nanocomposites

PVA is a semicrystalline polymer and the degree of crystallinity of PVA matrix is a deterministic factor for its mechanical properties. XRD pattern of semicrystalline polymers can be used to evaluate their relative crystallinity. XRD patterns of pure PVA and the nanocomposite films are plotted in figure 7 which shows the characteristic broad diffraction peak ($2\theta \sim 19^o$) for PVA. In order to evaluate the relative crystallinity, the broad diffraction peak is fitted to a combination of two Gaussian peaks representing the diffraction from amorphous region (broad peak) and crystallites (narrow peak). The fractional area under the narrow peak (narrow/broad+narrow) is calculated as relative crystallinity. Thus calculated crystallinity is shown in figure 8 indicating a continuous decrease in crystallinity as a result of GO loading. The melting points of PVA crystallites were measured using DSC as shown in figure S3*(ESI)*. The figure shows that melting point of PVA crystallites are not changed with nanocomposite formation indicating that the crystallite size is not altered while their number is reduced in the matrix resulting in a decrease in crystallinity.[32] The XRD pattern of the nanocomposites also do not show any diffraction peak corresponding to the GO indicating that GO is completely exfoliated in PVA matrix. The exfoliation of GO in polymer matrix was also confirmed from SEM micrographs of fractured surfaces of the nanocomposites (Figure 9). No signature of GO aggregates is observed from the micrographs. The observations from XRD and SEM confirm that the GO sheets are dispersed at molecular level in the PVA matrix.

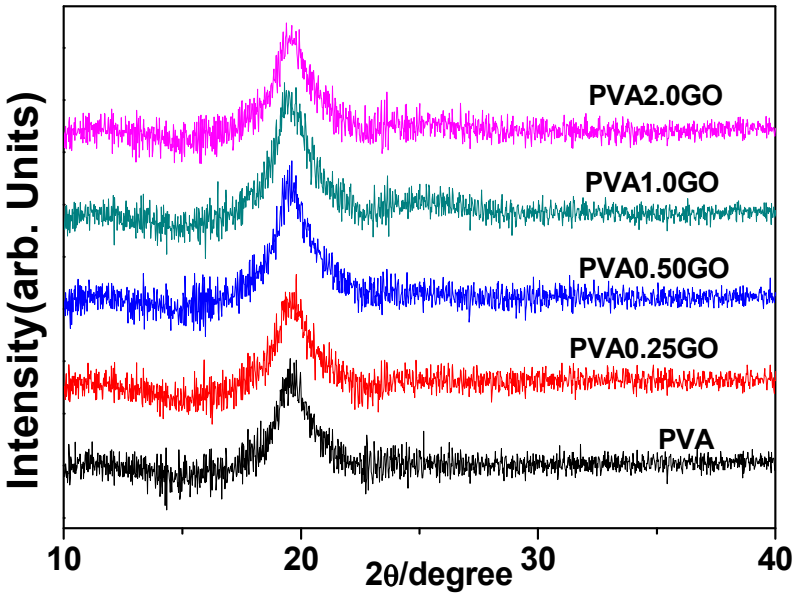

Figure 7. *XRD pattern of PVA-GO nanocomposites*

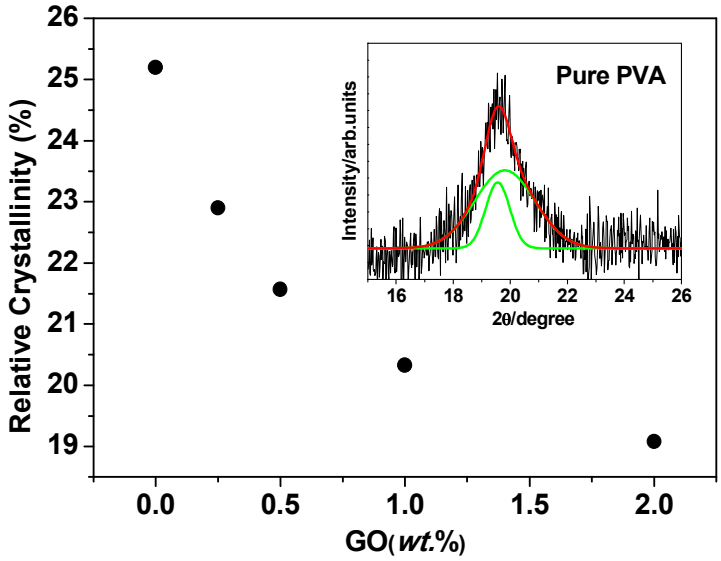

Figure 8. *Relative crystallinity of PVA nanocomposites evaluated from XRD patterns*

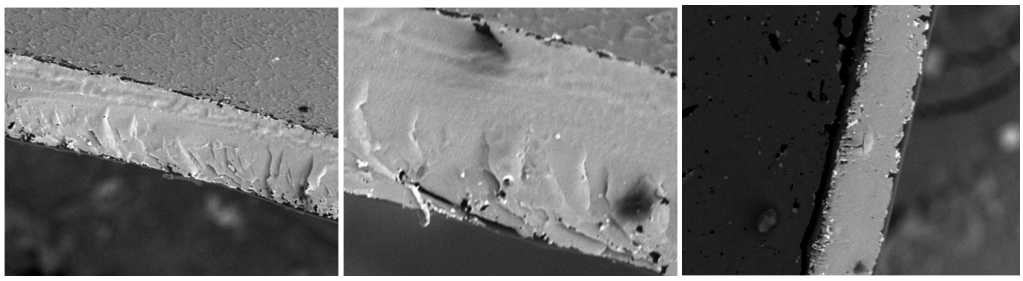

Figure 9. *SEM of fractured surfaces of (a) pure PVA (b) PVA-0.5GO and (c) PVA2.0GO*

The changes in molecular packing (sub nano level) of the nanocomposites have been characterized using PALS measurements. PALS spectra of GO, pure PVA and the nanocomposites were analyzed using PATFIT-88[33] and the results are reported in Table 2. Three discrete lifetime components (τ_i, i = 1,2,3) and corresponding intensity (I_i) evaluated from PATFIT analysis are ascribed to *p*-Ps , free positron and *o*-Ps *pick-off* annihilation in the samples. It is observed from the data that *o*-Ps lifetime, τ_3 (radius of the free volume holes) and corresponding intensity, I_3 (density of nanoholes) vary as a result of GO incorporation in the PVA matrix. Under such scenario, the fractional free volume provides superior information rather than the variation in *o*-Ps lifetime or intensity as individual parameters. The relative fractional free volume F_v is calculated using equation 2

$$F_v = I_3(4\pi R^3/3) \quad (2)$$

where R (nm) is the radius of free volume hole determined from *o*-Ps lifetime using equation (1) and I_3 (percentage) is the corresponding intensity. Thus calculated F_v is plotted in figure 10. The figure shows that the F_v for nanocomposites is lower than pure PVA, and PVA0.25GO has the minimum free volume available out of the studied samples. The discrete component free volume analysis represent an average picture of modification in free volume hole size and density. According the conventional theories of polymer materials, the free volume nanoholes in polymer matrix surely have a size distribution around its mean which can be determined from PALS measurements. For this purpose, a computer program CONTIN[34] based on inverse Laplace transformation is used. The positron lifetime spectrum is expressed as Laplace transformation of a function $\alpha(\lambda)\lambda$ in CONTIN analysis. The function $\alpha(\lambda)$ is the probability density function (pdf) of inverse of *o*-Ps lifetime i.e. annihilation rate (λ). It is expressed as a Gaussian distribution according to equation 3

$$\alpha_i(\lambda)\lambda d\lambda = \frac{1}{\sigma\sqrt{2\pi}}\exp\left[-\frac{(\ln\lambda/\lambda_{i0})^2}{2\sigma^2}\right]d\lambda \quad (3)$$

The subscript i and parameter σ are the number of lifetime component and the standard deviation of the function. The pdf of annihilation rate or *o*-Ps lifetime can be transformed into nanohole's radii through equation 1. The radii distribution of pure PVA and PVA-GO nanocomposites are shown in figure 11 indicating that the distribution is narrowed down with GO loading. In our earlier studies, it has been shown that the size distribution of free volume nanoholes undergoes modifications as a result of nanocomposite formation.[21-25] In these studies it was observed that the nanohole distribution is mainly modified due to interaction between polymer molecule and the filler. In case of weak interaction between polymer molecule and nanofillers, the radii distribution is converted to a bimodal distribution corresponding to two different spatial zone i.e. interphase and bulk polymer matrix. This has been clearly shown using PALS in our previous studies on PVA-SiC nanofibre composites. In this study, it was shown that an interphase with higher size free volume holes is created around the SiC nanofibre due to its weak interaction (van der Waals) with PVA molecules. Thus created interphase was observed to be responsible for decrement of the load transfer from PVA molecules to the SiC nanofibres.[21] On the other hand, in case of strong interaction (hydrogen bonding or covalent bonding) between polymer molecule and nanofillers, the complete polymer matrix structure (molecular packing) is modified to accommodate the fillers in the matrix. The present study is similar to the latter case and the observed variation in radii distribution indicates a strong interaction between PVA molecules and GO. This is highly possible due to the presence of functionalities on GO surface which can interact with hydroxyl groups presents in PVA backbone. In order to confirm the strong interaction between PVA and GO, variation in intensity (I_2) corresponding to free positron annihilation (second component from PALS analysis using PATFIT-88) has been compared to the calculated intensity according to simple mixture rule (Figure S4, *ESI*). The positive deviation observed in I_2 from the calculated values confirms the strong interaction between PVA molecule and GO sheets. The strong interaction between PVA and GO sheets has also been confirmed using FT*IR*. The presence of a peak at 1701 cm^{-1} for nanocomposite samples confirms the presence of GO in the nanocomposite samples. FT*IR* spectra of pure PVA and the nanocomposite films are shown in figure 12. The broad and strong absorption at ~3200 cm^{-1} corresponds to –OH stretching in PVA and

any change in this band indicate the change in hydrogen bonding between PVA molecules. From FT*IR* spectrum, a decrease (3201 and 3175 cm^{-1} for pure PVA and PVA2.0GO, respectively) in –OH stretching indicates the reduction in hydrogen bonding between PVA molecules. This happens because many –OH groups from PVA undergo hydrogen bonding with GO sheets due to availability of functional groups on its surface.

Table 2. *Positron annihilation lifetime analysis data for GO, pure PVA and PVA-GO nanocomposites*

Sample	τ_2(ns) error≤0.006 ns	I_2 (%) error ≤ 3.2%	τ_3(ns) error≤0.01ns	I_3(%) error≤0.45%
GO	0.369	73.5	---	---
Pure PVA	0.412	36.6	1.45	20.66
PVA0.25GO	0.355	47.7	1.40	19.56
PVA0.50GO	0.397	39.2	1.42	19.88
PVA1.0GO	0.403	38.7	1.44	19.01
PVA2.0GO	0.471	38.7	1.47	19.58

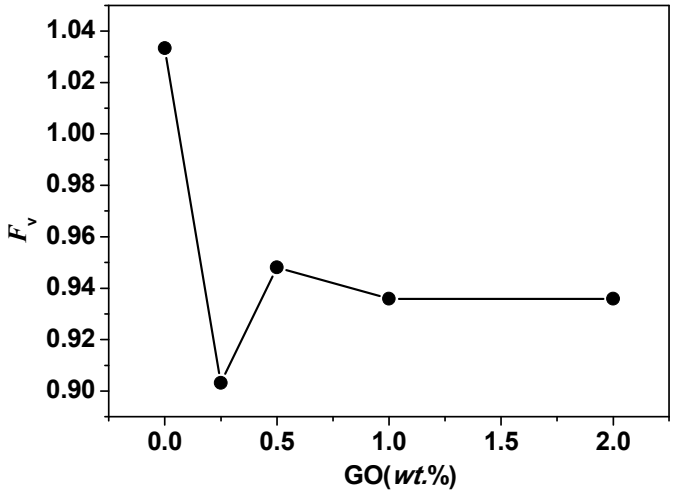

Figure 10 : Fractional free volume in PVA-GO nanocomposite as a function of GO loading (*wt.*%)

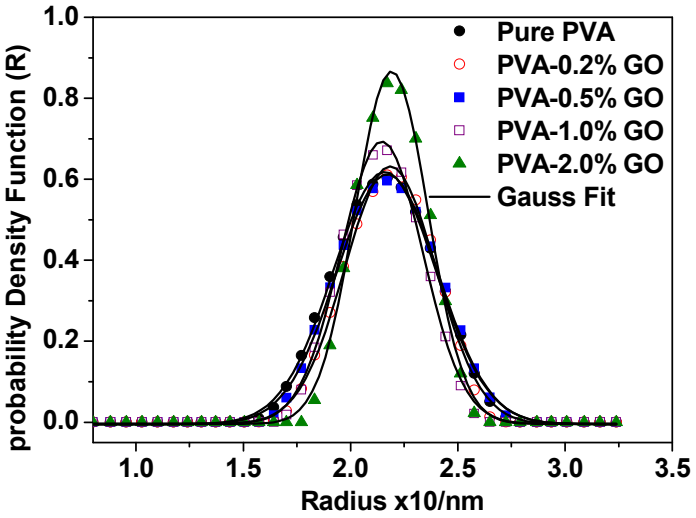

Figure 11. Free volume holes radius distribution in PVA-*x*GO nanocomposites.

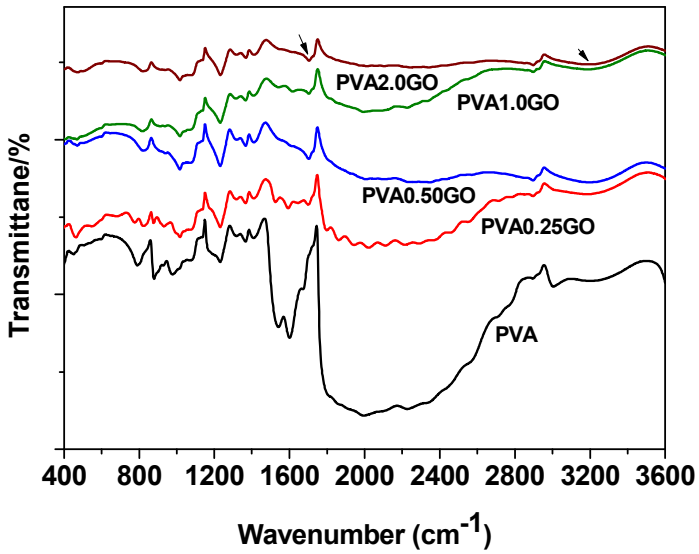

Figure 12. *FT*IR spectra of pure PVA and PVA-GO nanocomposite

4. Discussion

In the present study, contrary to our expectations, the mechanical properties are seen to be hampered on inclusion of GO in PVA matrix (Figure 4 and Table 1). This observation is also supported from fractured surface SEM morphology of the nanocomposites (Figure 9). The roughness observed at the fractured surface of pure PVA is highly reduced for

2.0% GO loading indicating the enhancement in brittleness of the nanocomposite films. In literature, enhancement in mechanical properties has been reported for PVA nanocomposites with various carbon nanofillers such as GO[13-17], r-GO, functionalized MWCNTs etc.[1,4-10] As mentioned before, the mechanical properties are heavily dependent on crystallinity, load transfer from PVA to GO sheets, molecular packing of PVA molecules in amorphous region (free volume nanohole parameters). It has been confirmed from XRD and SEM (Figures 7 and 9) that GO sheets are fully exfoliated and highly dispersed in PVA matrix. In such a case, efficient load transfer is expected from PVA molecule to GO sheets. Again, hydrogen bonding interaction between PVA molecule and GO has been established from *FT*IR and supported by PALS. This type of interaction facilitates the load transfer between PVA molecule and GO. The molecular packing in the amorphous region of PVA appears to be associated with narrower distribution of free volume nanoholes with a relatively lower free volume fraction as compared to pure PVA (Figures 10 and 11). According to conventional theories, the mechanical properties have inverse correlation with the free volume fraction of polymer. This is mainly because presence of a free volume hole act as a weak point in the matrix and it restricts the load transfer among polymer molecules leading to inferior mechanical properties. In the present case, the evolved molecular packing favours the improvement in the mechanical properties of the nanocomposite which is again in contradiction to the mechanical testing parameters observation. Hence the only remaining parameter i.e. crystallinity appears to be a deterministic parameter for governing the mechanical properties.

The crystallinity of the nanocomposite samples have been evaluated from their XRD patterns (Figure 8) and a continuous decrease in crystallinity has been observed with GO loading. The reduction in crystallinity seems to be responsible for the observed decrease in mechanical properties. As shown from PALS and *FT*IR, GO can interact with PVA molecule through hydrogen bonding leading to a complete change of PVA matrix (Figures S4 and 12). GO inclusion in PVA matrix brings two primary changes (i) it reduces the hydrogen bonding between PVA molecules and (ii) it acts as a physical barrier to PVA molecules restricting their dynamical motion. Both of these effects finally restrict the PVA molecules, especially in the vicinity of GO sheets, to undergo an ordered arrangement which is necessary for the crystallite formation in PVA matrix. The PVA loading in these samples has limited to maximum 2.0 wt.% which corresponds to 1.44 vol% (density of PVA and GO are 1.3 and 2.2 g/cc).[5] At such low concentration of GO, a large volume fraction of PVA remains unaffected and hence similar size crystallites with

their smaller number are produced as inferred from XRD and DSC measurements (Figures 7 and S3).

In literature, significant enhancement in mechanical properties for PVA-GO nanocomposites has been reported.[5-7,13,14,16] The observed enhancement has been ascribed to efficient load transfer from PVA to GO sheets as the variation in crystallinity with GO loading was shown to be either improved or unaffected. Xu et al.[4] and Liang et al.[5] have shown 62 and 162% enhancement in Young's modulus for PVA-GO nanocomposites while the crystallinity was shown to be nearly unaffected. In these studies, the highest value of Young's modulus for 2.0% GO loading is 3.8GPa which is lower than the Young's modulus of pure PVA reported in other reports (~ 4.5 GPa) [6,12] as well as present study (4.4 GPa). The crystallinity of PVA nanocomposite films prepared by Liang et al.[5] was in the range of ~ 18.0% which is less as compared to crystallinity of pure PVA films in the present study. This shows that crystallinity of pure PVA and its variation with filler loading plays a deciding role in mechanical properties.

As discussed earlier, the changes in crystallinity and molecular packing also affect the thermal properties of the nanocomposites. TGA data (Figure 5 and Table 1) show that the elimination of water as a result of loss of –OH functionalities becomes slower in GO loading. It is shown from *FT*IR and PALS data that PVA molecules interact with GO sheets through hydrogen bonding. This new hydrogen bonding is responsible for reducing the rate of mass loss corresponding to second step. This new hydrogen bonding also reduces the original hydrogen bonding in PVA matrix and consequently a small decrease in T_g is also observed [Figure 6 and Table 1]. The GO loading in PVA matrix structure is also shown to facilitate the mass loss corresponding to elimination of organic volatile. The reduced hydrogen bonding in PVA matrix has reduced the T_g of the matrix indicating that the diffusion of volatiles through PVA matrix would be facilitated in the composite resulting in a faster mass loss corresponding to pyrolisation of PVA backbone.

Conclusion

The present study shows that as a result of strong hydrogen bonding between PVA molecules and GO sheets, the nanofillers i.e. GO can be dispersed at molecular level in PVA matrix using simple aqueous solution casting method. The crystallinity of PVA was observed to reduce with GO loading primarily due to the restricted dynamical motion of the bonded PVA molecules. The strong interaction between PVA and GO was also

observed to reduce the original hydrogen bonding between PVA molecules resulting in lower free volume fraction with narrower free volume hole size distribution. The net effect of these variations in crystallinity and molecular packing are the deterioration in mechanical (reduction in Young's modulus) and thermal (reduction in T_g) properties. Comparison with literature reports reveals that crystallinity of pure PVA and the nanocomposites films is a deterministic factor for evolution of mechanical properties. Hence, in order to achieve the superior mechanical properties, there is a need of improvement in nanocomposite preparation method by which PVA-GO nanocomposite films with improved molecular packing and higher crystallinity can be prepared while dispersing GO sheets at molecular level with its highest possible concentration.

References

1. C. Zhang, S. Huang, W. Wei Tiju, W. Fan and T. Liu, *J. Mater. Chem.*, 2012, **12**, 2427-2434.
2. H. J. Salavangione, G. Martinez and M. A. Gomez, *J. Mater. Chem*., 2009, **19**, 5027-5032.
3. J. Y. Xu, Y. Hu, L. Song, Q. G. Wang, W. C. Fan, G. X. Lio and Z. Y. Chem, *Poly. Deg. Stab.*, 2001, **73**, 29-31.
4. Y. Xu, W. Hong, H. Bai, C. Li and G. Q. Shi, *Carbon*, 2009, **47**, 3538-3543.
5. J. J. Liang, Y. Hunag, L. Zhang, Y. Wang, Y. F. Ma, Y. Y. Guo and Y. S. Chen, *Adv. Fun. Mater.*, 2009, **19**, 2297-2302.
6. C. Bao, Y. Guo, Li. Song and Y. Hu, *J. Mater. Chem.*, 2011, **21**, 13942-13950.
7. Y. Li, T. Yang, T. Tu, L. Zheng and K. Liao, *J. Mater. Chem.*, 2011, 21, 10844-10851.
8. W-L. Song, W. Wang, L.M. Veca, C. Y. Kong, M-S. Cao, P. Wang, M. J. Meziani, H. Qian, G. E. Lecroy, L. Cao and Y-P. Sun, *J. Mater. Chem.*, 2012, **22**, 17133-17139.
9. Y. Wang, Z. Shi and J. Yin. *J. Phys. Chem. C*, 2010, **114**, 19621-19628.
10. J. Han, Y. Dou, D. Yan, J. Ma, M. Wei, D. G. Evans, X. Duan, *Chem. Commun.*, 2011, **47**, 5274-5276.
11. S. Pandey, S. K. Pandey, U. Parasher, G. K. Mehrotra and A. C. Pandey, *J. Mater. Chem.*, 2011, **21**, 17154-17159.
12. Y. Hou, J. Tang, C. Quian, Y. Feng and J. Liu, *ACS Nano*, 2009, **3**, 1057-1062.

13. L. Zhang, Z. Wang, C. Xu, Y. Li, J. Gao, W. Wang and Y. Liu, *J. Mater. Chem.,* 2011, **21**, 10399-10406.
14. L. Liu, Y. Gao, Q. Liu, J. Kunag, D. Zhou, S. Ju, B. Han and Z. Zhang, *Small*, 2013, **9**, 2466-2472.
15. K-J. Lin, S-C. Lee and K. F. Lin, *J. Polym. Res*., 2014, 21, 611(1)-(4).
16. H. K. F. Cheng, N. G. Sahoo, Y. P. Tan, Y. Pan, H. Bao, L. Li, S. H. Chan and J. Zhao, *ACS Appl. Mater. Inter.,* 2012, 4, 2387-2394.
17. M. M. J. Trecay, T. W. Ebbesen and J. M. Gibson, *Nature*, 1996, **381**, 678-680.
18. J. T. Paci, T. Belytschko and G. C. Schatz, *J. Phys. Chem. C,* 2007, 11, 18099-18111.
19. C. Gomez Navarro, M. Burghard and K. Kern, *Nano Lett.*, 2008, **8**, 2045-2049.
20. X. Zhao, Q. H. Zhang, D. J. Chen and P. Lu, *Macromolecules*, 2010, **43**, 2357-2363.
21. S. K. Sharma, J. Prakash, K. Sudarshan, D. Sen, S. Mazumder and P. K. Pujari, *Macromolecules*, 2015, **48**, 5706-5713.
22. S. K. Sharma, J. Prakash, K. Sudarshan, P. Maheshwari, D. Sathiyamoorthy and P. K. Pujari, *Phys. Chem. Chem. Phys.*, 2012, **14**, 10972-10978.
23. S. K. Sharma, J. Bahadur, P. N. Patil, P. Maheshwari, S. Mukherjee, K. Sudarshan, S. Mazumder and P. K. Pujari, *Chem. Phys. Chem*., 2013, **14**, 1055-1062.
24. S. K. Sharma, J. Prakash, J. Bahadur, K. Sudarshan, P. Maheshwari, S. Mazumder and P. K. Pujari, *Phys. Chem. Chem. Phys.,* 2014, **16**, 1399-1408.
25. P. N. Patil, K. Sudarshan, S. K. Sharma, P. Maheshwari, S. K. Rath, M. Patri and P. K. Pujari, *Chem. Phys. Chem.* 2012, **13**, 3916-3922.
26. S. Harms, K. Ratzke, F. F. Gerald, J. Schneider, L. Willner and D. Richter, *Macromolecules*, 2010, **43**, 10505-10511.
27. R. Zaleski, A. Kierys, M. Grochowicz, M. Dziadosz and J. Goworek, *J. Colloid Interface Sci*. 2011, **358**, 268-276.
28. S. Awad, H. Chen, G. Chen, X. Gu, J. L. Lee, E. E. Abdel-Hady and Y. C. Jean, *Macromolecules*, 2011, **44**, 29-38.
29. S. J. Tao, *J. Chem. Phys*., 1972, **56**, 5499-5510.
30. M. Eldrup, D. Lightbody and J. N. Sherwood, *Chem. Phys*., 1981, **63**, 51-58.
31. P. S. Thomas, J.-P. Guerbois, G. F. Russell and B. J. Briscoe, *J. Therm. Anal. Cal.,* 2001, **64**, 501-508.

32. R.S. Porter and L-Hui Wang, *J. Therm. Anal.*, 1996, **46**, 871-878.

33. P. Kir kegaard and M. Eldrup, *Comput. Phys. Commun*., 1991, **17**, 401-409.

34. S. W. Provencher, *Comput. Phys. Commun*., 1982, **27**, 213-227.

Electronic Supplementary Information (ESI)

SEM-EDX measurements on GO powder; Determination of melting point of PVA-GO nanocomposites from heating cycle DSC thermogram; variation of free positron lifetime as a function of GO loading

Acknowledgement

Authors would like to thank Dr. Amit Srivastava, Dr. B. Paul and Dr. H. Sodaye from Bhabha Atomic Research Centre (BARC), Mumbai for carrying out the TEM, SEM and mechanical testing measurements.